Synthesis of Polyaniline/Multiwall Carbon Nanotube Composite via Inverse Emulsion Polymerization

DUK KI KIM,[1] KYUNG WHA OH,[2] SEONG HUN KIM[1]

[1]Department of Fiber and Polymer Engineering, Hanyang University, 17 Haengdang-dong, Sungdong-gu, Seoul 133-791, Korea

[2]Department of Home Economics Education, Chungang University, 221 Heukseok-dong, Dongjak-gu, Seoul 156-756, Korea

Received 26 December 2007; revised 8 July 2008; accepted 4 August 2008
DOI: 10.1002/polb.21557
Published online in Wiley InterScience (www.interscience.wiley.com).

ABSTRACT: The composite of polyaniline (PANI) and multiwall carbon nanotube carboxylated through acid treatment (c-MWCNT) was synthesized by chemical oxidative polymerization in an inverse emulsion system. The resultant composites were compared with products from aqueous emulsion polymerization to observe the improvements in electrical conductivity, structural properties, and thermal stability obtained by this synthetic method. Prior to the inverse emulsion polymerization, MWCNT was treated with a strong acid mixture to be functionalized with carboxylic acid groups. Carboxylic acid groups on surfaces induced selective dispersibility between polar and nonpolar solvents because of the increase of hydrophilicity. As the content of c-MWCNT was increased, the electrical conductivity was increased by a charge transport function from the intrinsic electrical conductivity of MWCNT and the formation of a highly ordered dense structure of PANI molecules on the surface of c-MWCNT. The images observed with electron spectroscopy showed the capping of c-MWCNT with PANI. The growth of additional ordered structures of PANI/c-MWCNT composite, which was observed through wide-angle X-ray diffraction patterns, supported the capping by PANI. It was observed that the doping of the composite had a significant relationship with the concentration of dodecylbenzenesulfonic acid (DBSA). The thermal stability of PANI composite was improved by the addition of c-MWCNT; this was thought to be related with structure ordering by inverse emulsion polymerization.
 J Polym Sci Part B: Polym Phys 46: 2255–2266, 2008
Keywords: conducting polymer; emulsion polymerization; inverse emulsion polymerization; multiwall carbon nanotube; nanocomposites; polyaniline

INTRODUCTION

Polyaniline (PANI) is a promising material because of its intrinsic electrical conductivity by doping with organic dopants.[1–3] PANI doped with anionic dopants has been developed for organic conducting additives, which were applied as electronic actuators, charge transport agents in a polymer matrix, and electromagnetic interference shielding materials.[4–6] Recently, these conducting particles were also used as organic circuitry through the lithography or mold compression methods.[7,8] However, most synthetic conducting polymers doped with anionic surfactants have a limit on electrical conductivity. The ideal conducting

Correspondence to: S. H. Kim (E-mail: kimsh@hanyang.ac.kr)

polymer single molecule with π-conjugated structure is expected to have metal-like electrical conductivity generated by intramolecular charge transfer. Although intermolecular charge transport is possible by hopping of electrons through overlapping π-orbitals, at this point, intermolecular charge transport has a more significant relationship with electrical conductivity. Therefore, highly ordered structures such as crystalline or self-assembled structures have revealed excellent electrical conductivity.[9,10] The limitation of electrical conductivity is also caused by dedoping of the conducting polymer, which can occur through decomposition by heat or desorption from the polymer chain. The highly ordered structure interrupts desorption of dopant molecules from the polymer chain by mechanical entrapment. To induce an ordered structure, other materials acting as a template for the composite are required.

As a template for adsorption of PANI, carbon nanotube (CNT)[11] was selected. CNT has attracted a great deal of interest, both as advanced reinforcement[12–14] and in a wide range of electronic industrial applications.[15] Its graphite structure with high-chemical stability during synthesis, its mechanical endurance under ultrasonication, and its electrical conductivity make CNT well suited to synthesizing a PANI/CNT composite. However, pristine CNT has no functional group to develop dispersibility in organic polar solvents and a polar interaction between the CNT and the polymer matrix. Thus, specific modifications were required through vigorous oxidation methods on the surface of the CNT, such as acid treatment or plasma treatment. A typical method to prepare PANI/multiwall carbon nanotube (MWCNT) composites is *in situ* aqueous solution polymerization or emulsion polymerization.[16–21] Especially, Wu and Lin[16] and Wan and coworkers[17] reported significant results in their articles through functionalization of MWCNT and polymerization of PANI on the surface of MWCNT.

Recently, a novel process for synthesis of PANI using a water in oil (W/O) system, designated "inverse emulsion polymerization," has been studied.[22–27] In this method, the mechanism of polymerization and assembly of molecules is different from that in aqueous emulsion polymerization, as shown in Figure 1. The method has good potential to produce PANI/carboxylated MWCNT (c-MWCNT) composites, because c-MWCNT exhibits different dispersibility according to types of solvent, aqueous media and hydrocarbon media. The c-MWCNT has more affinity with water than with hydrocarbon. This selectivity is caused by the functionalization of MWCNT with carboxylic acid groups and makes it possible to transfer c-MWCNT into water in the inverse micelle. Moreover, Han et al.[28] reported the assumption that the synthesized PANI molecules doped with dodecylbenzenesulfonic acid (DBSA) remained in water droplets that are stably dispersed by DBSA in the W/O system. Therefore, it was expected that the probability of adsorption of PANI on c-MWCNT could increase, and the structure order could be controlled better in the W/O system than in the aqueous emulsion system, because the synthesized polymer propagates in the direction of the water, and there is interaction between the carboxyl group and the amine groups of PANI. In brief, this study is based on two major concepts, the adsorption mechanism of PANI molecules on c-MWCNT in water droplets and the existence of an attracting force between PANI molecules and surface of c-MWCNT.

The purpose of this research is to develop more stable and durable conducting materials with higher conductivity than conducting polymer/CNT composites synthesized using aqueous emulsion polymerization. The aggregation of polymer particles can be relieved because aniline monomer is provided from the oil phase through the interface stabilized by surfactant to the aqueous phase containing an oxidant for initiation and radical coupling site of PANI for propagation. The highly ordered structure of PANI has advantages for the electrical and thermal properties and durability of the particles. The creation of well dispersed, small-sized particles, and the regular size distribution of the composite particles are expected to have a good effect on applications with other polymers as the organic conducting filler.

EXPERIMENTAL

Materials

MWCNT was purchased from Il-jin Nanotech Co., Ltd. (CM95, purity >95%, length 10–50 μm, diameter 10–30 nm). MWCNT synthesized via the chemical vapor deposition (CVD) method.[29–31] Sulfuric acid (99%, Sigma-Aldrich Chemical Co.), nitric acid (70%, Sigma-Aldrich), and ammonium persulfate (APS) were used without any treatment. For its purification, aniline (Sigma-Aldrich) was distilled under reduced pressure (69 °C/10

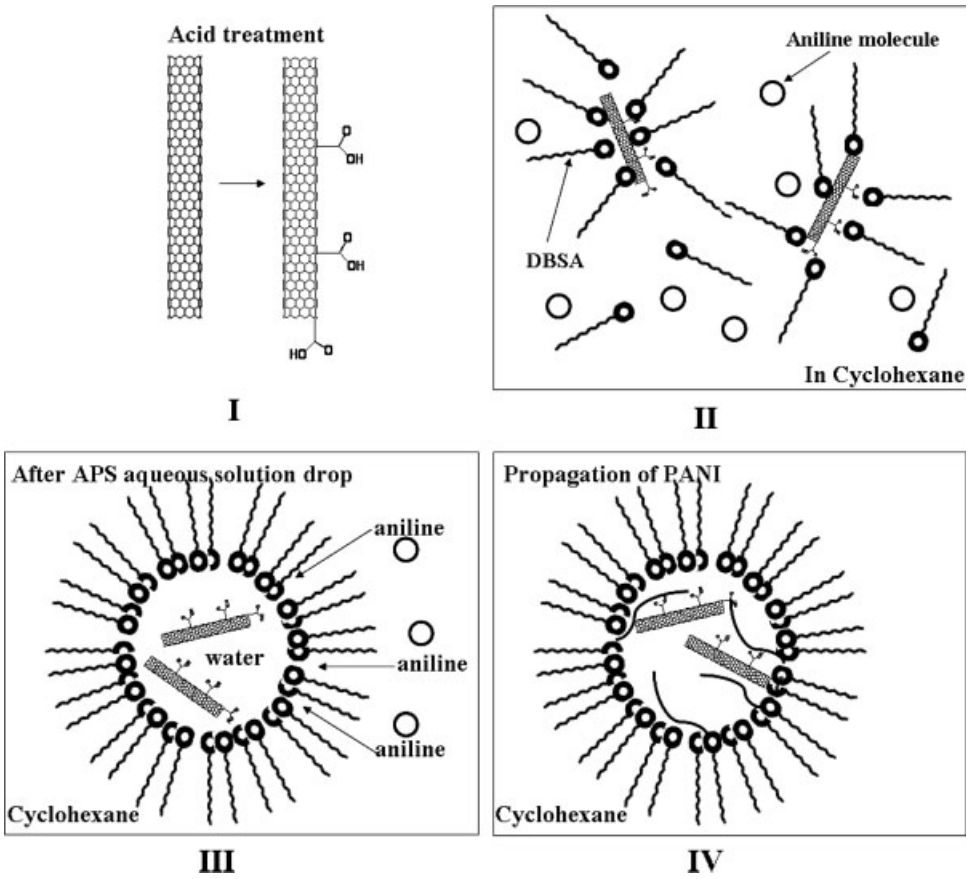

Figure 1. Schematic representation of the synthesis of PANI/c-MWCNT composite in inversed micelle.

mmHg). The selection of surfactant was more difficult than in the aqueous system because of the low-solubility parameters of cyclohexane (16.8 $MPa^{1/2}$). Most anionic surfactants such as naphthalenesulfonic acid or *p*-toluenesulfonic acid were not soluble or only partially soluble in hydrocarbon media. Referring to the theoretical hydrophile–liphophile balance value and chemical structures with long alkyl chains exhibiting hydrophobicity,[32] DBSA solution in isopropylalcohol (70 wt %) was used as a surfactant. Other solvents such as cyclohexane and methyl alcohol were used as supplied by Junsei Chemical Co.

Acid Treatment of MWCNT

MWCNT was suspended in a 3:1 mixture of concentrated H_2SO_4 and HNO_3 by ultrasonication. The solution was magnetically stirred and heated at 60 °C for 24 h. This treatment provides carboxylic acid groups at defects in the surface of tubes and exfoliates graphite.[20,33] Carboxyl modification on surfaces and breaking at defects increased the solubility of MWCNT in organic solvent and water.[33,34]

Synthesis of PANI/c-MWCNT Composites via Inverse Emulsion Polymerization

The composite of PANI/c-MWCNT was synthesized by chemical oxidative polymerization in an inverse emulsion system (W/O) as shown in Figure 1. Cyclohexane was selected as the medium for polymerization. Synthesis of PANI/c-MWCNT composite was subdivided into four steps. Figure 1 shows the Step (I) of modification by acid treatment. In Step (II), c-MWCNT is dispersed in cyclohexane containing DBSA with ultrasonication. In a typical experiment, DBSA was added to a 100 mL round-bottomed flask containing 50 mL of cyclohexane. (The standard solvent for molarity of each surfactant is the medium for polymerization, cyclohexane.) The concentrations of DBSA were varied from 0.01 M to 1.0 M. After 3 h magnetic stirring, c-MWCNT was introduced to the solution with ultrasonication. DBSA enclosed the

partially hydrophilic surface of c-MWCNT, which made it possible for the c-MWCNT to be dispersed in the cyclohexane medium. Then, aniline (0.1 mol/L) was added dropwise to the dispersion. In Step (III), to prepare the oxidizing solution, 0.1 mol/L APS was dissolved in distilled water with magnetic stirring for 1 h. Then, 10 mL of the aqueous solution was added dropwise to the mixture with mechanical stirring for 10 h. Continuous stirring and slow oxidant feeding was required to form a well-dispersed inverse emulsion system, because the large difference in solubility parameters between water and cyclohexane induced phase separation. As soon as the oxidizing solution was added, hydrophilic c-MWCNT could be hydrated by water and inverse micelles were formed in the W/O system.

In Step (IV), at the interface of the water and oil, polymerization of aniline was initiated through oxidation by APS. Two processes, formation of inverse micelles and initiation of polymerization by oxidation of monomer, occurred simultaneously in Steps (III) and (IV). Polymerization was carried out at 5 °C for 24 h. Finally, the PANI doped with DBSA propagates by radical coupling in the water medium and is adsorbed on the surface of c-MWCNT.

To terminate the reaction and remove cyclohexane, the polymer dispersion was poured into 1 L of methyl alcohol. The solution was filtered using a poly(tetra fluoroethylene) filter (d: 0.1 μm) under reduced pressure. Then, washing with distilled water and filtering were repeated for three times. Greenish polymer powders were dried in a vacuum oven at 50 °C for 24 h.

PANI/c-MWCNT Composite via Aqueous Emulsion Polymerization

To prepare a reference sample, aqueous emulsion polymerization was carried out. The synthetic method was similar to that used in our previous research.[35] DBSA (0.2 mol/L) and 0.1 mol/L of aniline were introduced into a 100-mL round-bottomed flask containing 50 mL of water. After 3 h vigorous stirring, c-MWCNT (5 wt % of aniline) was added to the emulsion with ultrasonication. Then, the same content of APS aqueous solution as for inverse emulsion polymerization was added dropwise with mechanical stirring over 10 h. After 24 h of reaction, the product was washed with methanol and distilled water under the same conditions as the inverse emulsion system.

Characterization

Field-emission scanning electron microscopy (FE-SEM; JEOL JSM-6330F, Tokyo, Japan) was used to determine the morphology of the prepared PANI/c-MWCNT composite. To observe the growth of PANI on the surface of c-MWCNT, which acts as a substrate, samples of the dispersion were extracted from the reaction at different times (3, 6, 9, and 12 h). Each sample was observed using transmission electron microscopy (TEM; JEOL JEM-2000, Tokyo, Japan). To confirm an increase of crystallinity and structural effect of c-MWCNT on PANI, wide-angle X-ray diffraction (WAXD) data were collected with a Rigaku Denki D-Max 2000 instrument. The electrical conductivity of PANI/c-MWCNT composites doped with DBSA was measured by means of a four-probe method,[36] using a Keithly 238 high-current-source measuring unit at room temperature. The electrical conductivity was calculated using the eq 1 as follows:

$$\sigma(\mathrm{S/cm}) = \frac{\ln 2}{\pi \cdot t} \times \frac{I}{E} \approx 0.22/t \times \frac{I}{E} \qquad (1)$$

where, σ is electrical conductivity; t is the thickness of the sample; E is the voltage drop across the inner probes; and I is the current passing through the outer probes. Modification of MWCNT with carboxylic acid group was confirmed through the Fourier-transform infrared (FTIR) spectra (Nicolet 760 Magna IR spectrometer) using KBr discs. FTIR spectra of PANI/c-MWCNT composite doped with DBSA were also recorded. The influence of the doping effect of DBSA on PANI/c-MWCNT composites was observed through UV–Vis spectra using SCINCO *S*-4100 UV–Vis spectroscopy. Samples of composites were synthesized using different concentrations of DBSA (0.01, 0.05, 0.2, 0.5, and 1.0 M) to observe polaron peak shifting at different doping levels. Additional experiments with samples containing different amounts of c-MWCNT (0, 1, and 10 wt %) were also carried out using UV spectra to observe the effect of c-MWCNT content on the UV spectra of the samples. A thermogravimetric analyzer (TGA) was used to determine the thermal properties of the composites and to assess the effects of c-MWCNT on the thermal properties of PANI. The temperature was increased from room temperature to 800 °C at the rate of 10 °C/min in argon.

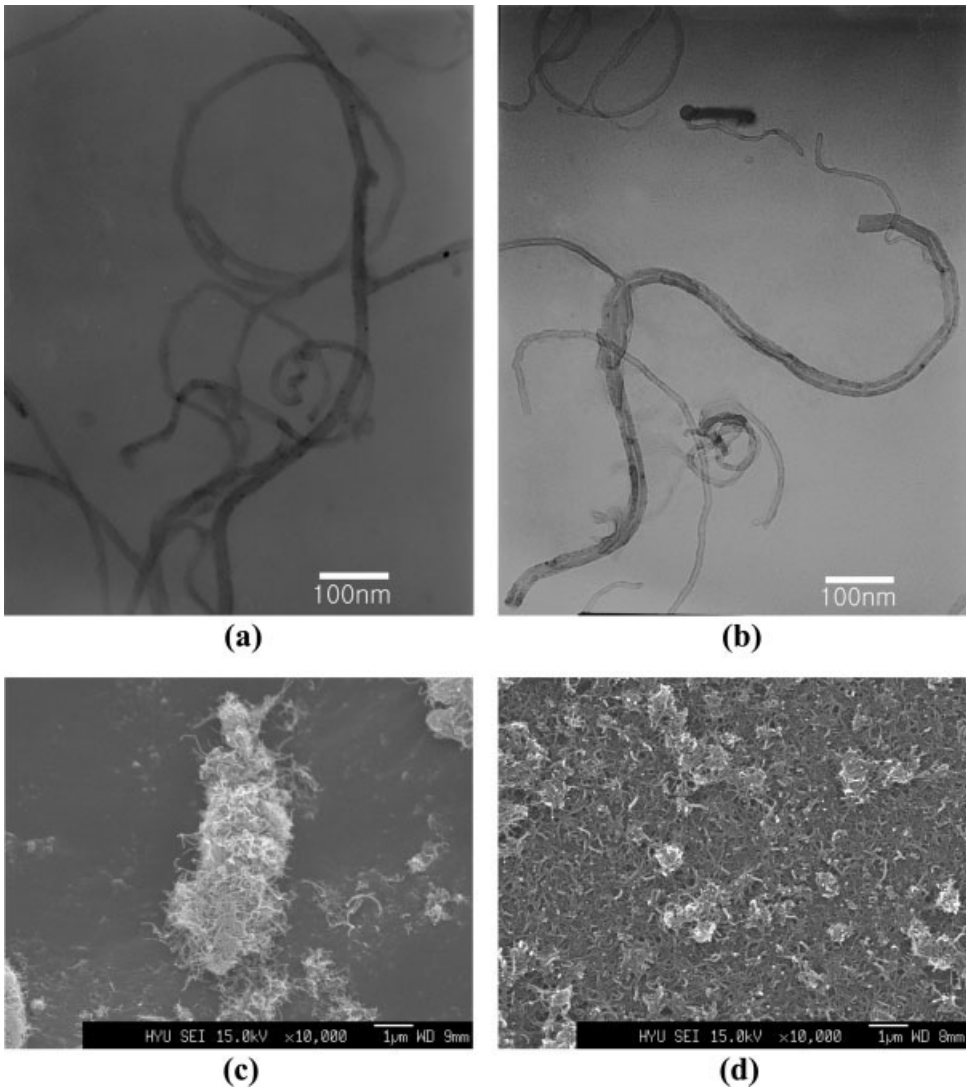

Figure 2. TEM image of MWCNT before (a) and after (b) acid treatment. SEM image of dispersed MWCNT in DMF before (c) and after (d) acid treatment.

RESULTS AND DISCUSSION

Carboxylated MWCNT

Prior to the synthesis, MWCNT is required to satisfy conditions such as dispersibility in the medium, short lengths to minimize coiling and removal of impurities. Acid treatment with a mixture of strong acids functionalizes the surface of MWCNT with carboxylic acid groups, carboxyl groups, and hydroxyl groups. Defects developed during the functionalization break the CNTs into short length. In Figure 2, c-MWCNT exhibited shorter lengths and a more purified form than pristine MWCNT. To observe dispersibility in the organic solvent, each sample of MWCNT before and after acid treatment was dispersed in DMF with sonication and each solution was dropped on a slide glass. The dispersed shapes are shown in Figure 2(c,d). There were significant differences in length, dispersibility, purity, and degree of coiling.

Some researchers have carried out *in situ* polymerization of conducting polymers based on MWCNT without any functionalization of the CNTs.[22] However, in inverse micelle polymerization, affinity of MWCNT to water was required to solubilize it into the water-phase in micelles. The treatment with a mixture of sulfuric and nitric acids provided functionality on hydrophobic MWCNT and made it possible for the functionalized MWCNT to be more dispersible in the water

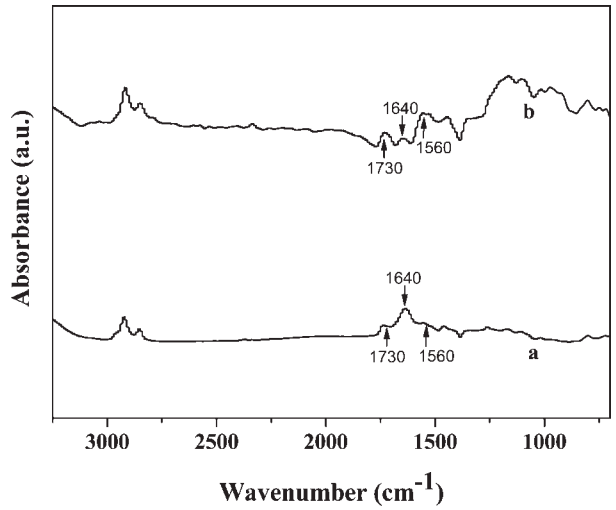

Figure 3. FTIR spectra of MWCNT (a) and c-MWCNT (b).

phase for long periods. Carboxyl functionalization was confirmed using the FTIR spectrum shown in Figure 3. In the spectrum of modified MWCNT, the C=O band appeared at 1560 cm^{-1} and the other weak band at 1730 cm^{-1} represents the carboxylic acid group. Compared with the spectrum of pristine MWCNT, the intensities of these two bands increased. Otherwise, the band of C=C vibration with sp^2 orbital decreased at 1640 cm^{-1}, which represents the graphite structure of MWCNT.

Effects of DBSA and c-MWCNT on the Electrical Properties of PANI/c-MWCNT

The electrical conductivities of PANI synthesized at several concentrations of DBSA and c-MWCNT are shown in Figure 4. To compare the inverse emulsion system with the aqueous system, the electrical conductivity of the product from the aqueous systems was also plotted. It can be seen that the optimum concentration of DBSA for synthesis was 0.2 M for these specimens. As shown in Figure 4, the electrical conductivity of PANI/c-MWCNT composite increased greatly with increasing c-MWCNT content, up to 5 wt %. In addition, the PANI/c-MWCNT composite exhibited better electrical conductivity than pristine PANI. This improvement may be explained by the high-electron transport capability of pristine MWCNT and the highly ordered structure of PANI formed on the surface of the MWCNT. For the PANI/c-MWCNT composite, the incorporated MWCNT can act as templates for the growth of PANI, thereby resulting in the function of MWCNT as charge carrier bridges in the core of particles for improving the electrical conductivity.

With each specimen of PANI/c-MWCNT composites, slight decrease in electrical conductivity was observed with concentrations of DBSA above 0.2 M. It is assumed that the decrease results from the aggregation of DBSA molecules near c-MWCNT at Step (I) in Figure 1. The excess DBSA interrupts the hydration of c-MWCNT and the approach of PANI molecules to the surface of the c-MWNCT. In addition, the solubilization of aniline monomers into the micelles can be delayed and interrupted.

Huang et al.[19] also suggested a doping effect associated with single-wall CNT. At the surface of the CNT, the formation of a more efficient matrix of conducting polymer for charge transport is believed to be induced. However, a doping effect by carboxylic acid groups substituted on c-MWCNT could not be confirmed. Therefore, UV–Vis spectroscopy and TEM were conducted to confirm the effect of introduced carboxylic group to MWCNT on the electrical conductivity of PANI/c-MWCNT.

To investigate UV–Vis absorption, 1.5 mg of each sample of PANI/c-MWCNT composite was dissolved in *m*-cresol with ultrasonication. It is known that three bands are observed at 350–365, 410–430, and 800–850 nm in PANI doped with DBSA. The peak at 350–365 nm is because of π–π^* transition of benzoid ring in the PANI structure in both doped and dedoped structures. The other peaks represent polaron absorption through organic doping. UV–Vis spectra of DBSA doped

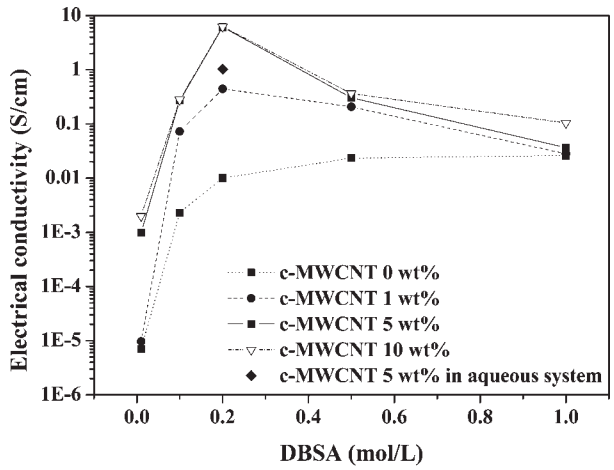

Figure 4. Electrical conductivity of PANI/c-MWCNT composites with different contents of DBSA and c-MWCNT.

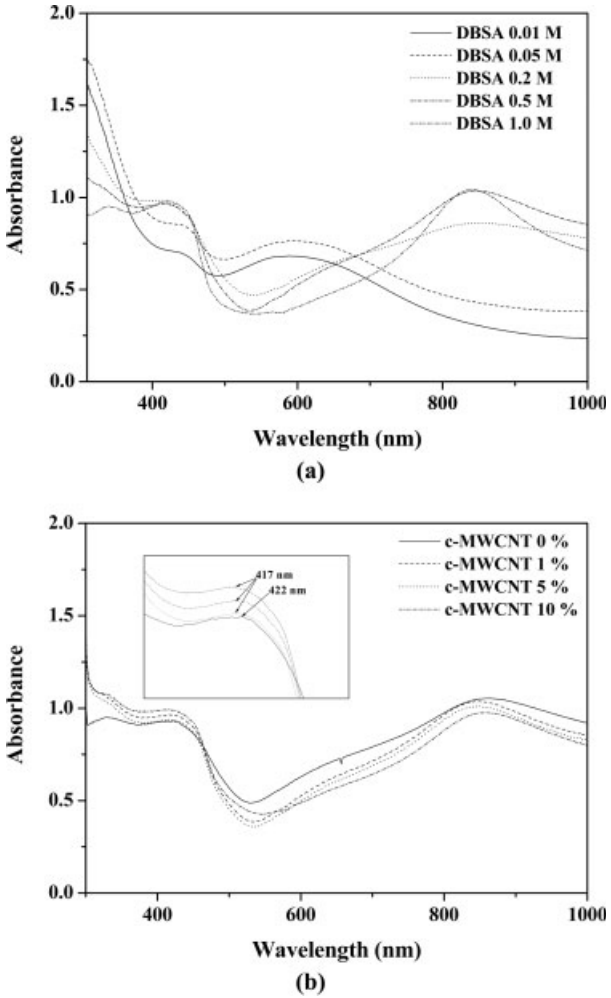

Figure 5. UV–vis spectra of PANI/c-MWCNT composites with different contents of DBSA (a) and c-MWCNT (b).

PANI containing 5 wt % c-MWCNT are shown in Figure 5(a). As the molar content of DBSA increased, the peak at 350–365 nm in the spectrum was reduced dramatically. A broad absorption also developed at around 600 nm and moved to 800 nm. The polaron band absorption was maximized when the composite was doped with 0.5 M DBSA (surfactant: monomer = 5:1). The concentration of DBSA at the highest doping did not agree with the optimum condition for electrical conductivity. The dissolving mechanism of PANI doped with DBSA is assumed to be the following. PANI/DBSA is a kind of charge transfer complex that consists of PANI cation and dopant anion.[37] Thus, it is possible that coulomb interaction between PANI and DBSA induces the approach of the polar solvent, *m*-cresol. From the interaction of solvent molecules, a partial loss in interaction between polymer and dopant is developed. Thus, the difference with other studies[38] may be reasonable. In our research, the resultant powders were washed and filtered with methanol and water. The solubilization of dopant from PANI matrix by solvent should be considered. As a result, it is concluded that the disagreement between concentration of DBSA exhibiting maximum polaron absorption and concentration of DBSA exhibiting maximum value of electrical conductivity could be caused by the dissolution of DBSA from the PANI matrix.

Samples with different concentrations of c-MWCNT were synthesized through inverse emulsion polymerization to observe the effect of the addition of c-MWCNT on UV–Vis absorbance. In Figure 5(b), there was little change of polaron absorption with different amounts of c-MWCNTs. From this experiment, it could be assumed that electrical conductivity did not result from the doping effect of MWCNTs functionalized with carboxylic acid but was significantly related to doping effects by the organic dopant. There was research to characterize the interfacial interaction between PANI and c-MWCNT in the core shell-type composite, which was synthesized in aqueous system.[39] In Figure 5(b), slight shift of polarlon-π transition peak from 422 to 417 nm was detected in PANI/MWCNT composite compared with PANI. This shift is assumed to be developed by the interaction between the quinoid rings of PANI and c-MWCNT. Wu and Lin also reported the similar results on UV–Vis spectra and discussed the adsorption mechanism by both hydrogen bonding and π–π interaction between carboxylated MWCNT and aniline monomer.

Other factors such as crystallinity, shape, or size of particles, and connection with MWCNTs must also be considered, because intermolecular charge transport as well as intramolecular charge transport makes a significant contribution to the conducting mechanism of the polymer. Consequently, c-MWCNT is assumed to act as a template for growth of PANI molecules by providing hydrogen bonding or π–π interaction.

Morphology and structures

Figure 6 shows images of PANI composite doped with 0.2 M DBSA, in which 5 wt % c-MWCNT was applied. This should be compared with the pristine c-MWCNT TEM image in Figure 2(b). Size variations in diameter and length of tubes were apparent, which were caused by both the

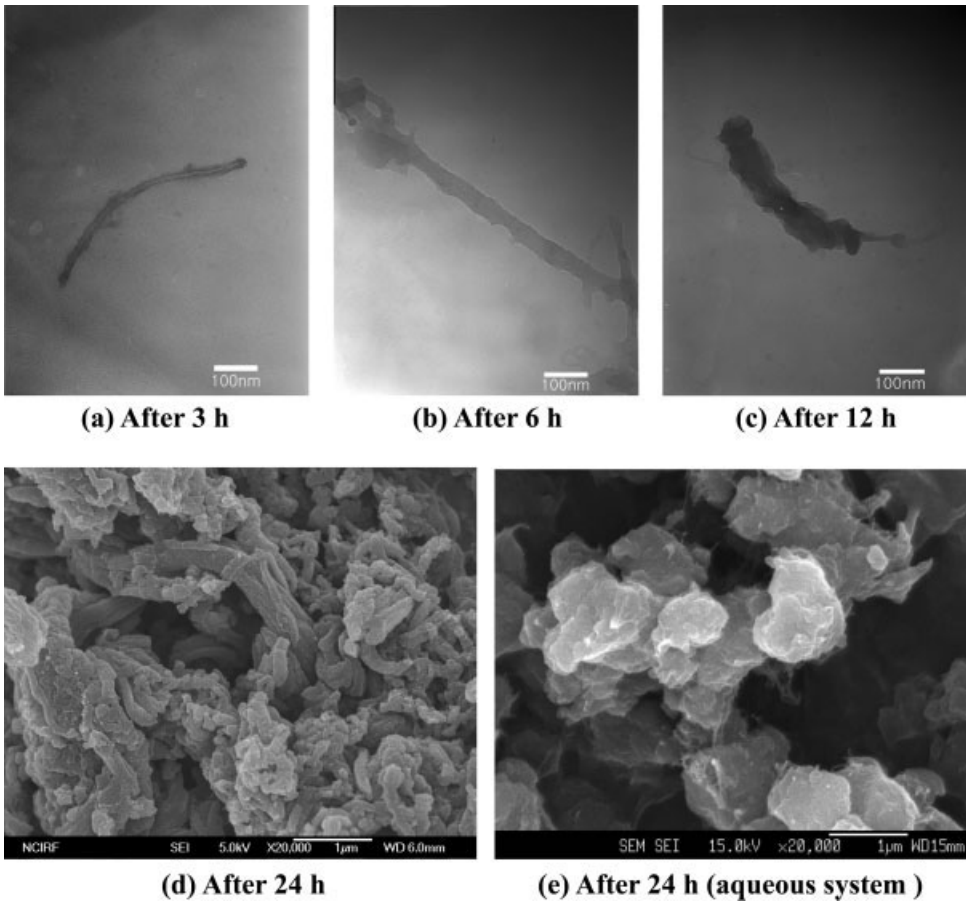

Figure 6. TEM image of PANI/c-MWCNT composites at difference reaction time (a), (b), and (c). SEM image of PANI/c-MWCNT composite particles after inverse emulsion polymerization (d) and aqueous emulsion polymerization (e).

original size distribution of MWCNT synthesized by a catalytic CVD process and cutting by acid treatment. To observe the capping process, the dispersions were extracted at intermediate stages of polymerization, and washed and dried. The dried powders were dispersed in dimethylformamide (DMF) with ultrasonication. The morphologies of the dispersed particles are shown in Figure 6(a–c) according to reaction time. The deposition of the PANI thin layer on the surface of the tubes was observed from the difference between the images of Figures 2(b) and 6(a). The deposition layer became thicker as the reaction time increased. As shown in Figure 6(a), it could be concluded that the capping of c-MWCNT resulting from adsorption of PANI molecules was not an irregular aggregation of PANI particles and tubes. The assumption of the existence of interaction between the surface of c-MWCNT and PANI is supported by these changes of morphology. As a result, it was assumed that PANI molecules form highly ordered structures on c-MWCNT that were not caused by simple aggregation between PANI particles and c-MWCNT. Consequently, PANI/c-MWCNT has the structure of a c-MWCNT core and a PANI shell, and this structure was developed from physical interactions such as π–π interaction between hexagonal structure of c-MWNCT and planar structure of PANI plentiful with π electrons. At the initial step of the synthesis, the capping mechanism can be explained as follows. When aqueous APS solution is dropped into c-MWCNT/DBSA/cyclohexane solution, DBSA molecules enclose the droplet and form an inverse micelle. The c-MWCNT is hydrated and penetrates into the water phase because the carboxylic acid group functionalized on MWCNT acts as a hydrophilic group and has an affinity with the water droplet in the inverse micelle. Aniline molecules approach the inverse micelle and the polymerization of PANI is initiated through oxidation by APS in the water phase. Then the PANI molecules

are propagated in the direction of the water phase and adhere to the surface of c-MWCNT, because the physical attracting force makes it possible for PANI molecules to deposit on surface of c-MWCNT.

On the other hand, as shown in Figure 6(e), c-MWCNT not enclosed by PANI could be observed at the edge of particles from the aqueous emulsion polymerization. From this image, it could be concluded that the products are developed from simple aggregation between PANI particles and c-MWCNTs in the case of aqueous emulsion method.

To characterize the relationship between the contents of c-MWCNT and the structure of composite, WAXD analysis was used as shown in Figure 7. On the pattern of pristine c-MWCNT, two diffraction peaks appeared at 25.9° (plane 002) and 43° (plane 111), which were developed from the graphite-like structure and catalytic particles inside the MWCNT.[40]

On the pattern of PANI doped with DBSA from inverse emulsion polymerization, the crystalline peaks were exhibited at 15.2°, 20.7°, 25.5°, 26.9°, and 29.8°. These peak positions are identified with the emeraldine salt form doped with HCl reported by Chaudhari and Kelkar.[10] Each peak represents a reflection plane (011), (020), (200), (121), and (022). The Bragg peaks near 25.5° and 20.7° (d spacings of 0.35 and 0.42 nm) are due to the π-staking distance between PANI chains and separation distance between lamellar by doped DBSA, respectively. In contrast to patterns of samples from the inverse emulsion polymerization, patterns of products from aqueous emulsion polymerization exhibited broad distribution of periodicity as determined from the band centered at 19.45°. This result supports the fact that the more highly ordered structure could only be developed through the inverse emulsion polymerization than aqueous emulsion polymerization. And also, a shift of the crystalline peak from 19.45° to 20.7° in the WAXD patterns indicates narrower interval among lattices. This result indicates that the PANI/c-MWCNT composites from inverse emulsion polymerization formed denser structures than the composite from aqueous emulsion polymerization. This dense structure has a significant relationship with the improvement of electrical conductivity from intermolecular charge transport as well as thermal stability.

The patterns of PANI/c-MWCNT composites (1, 5, and 10%) exhibited similar peak positions for PANI doped with DBSA except for the peak at

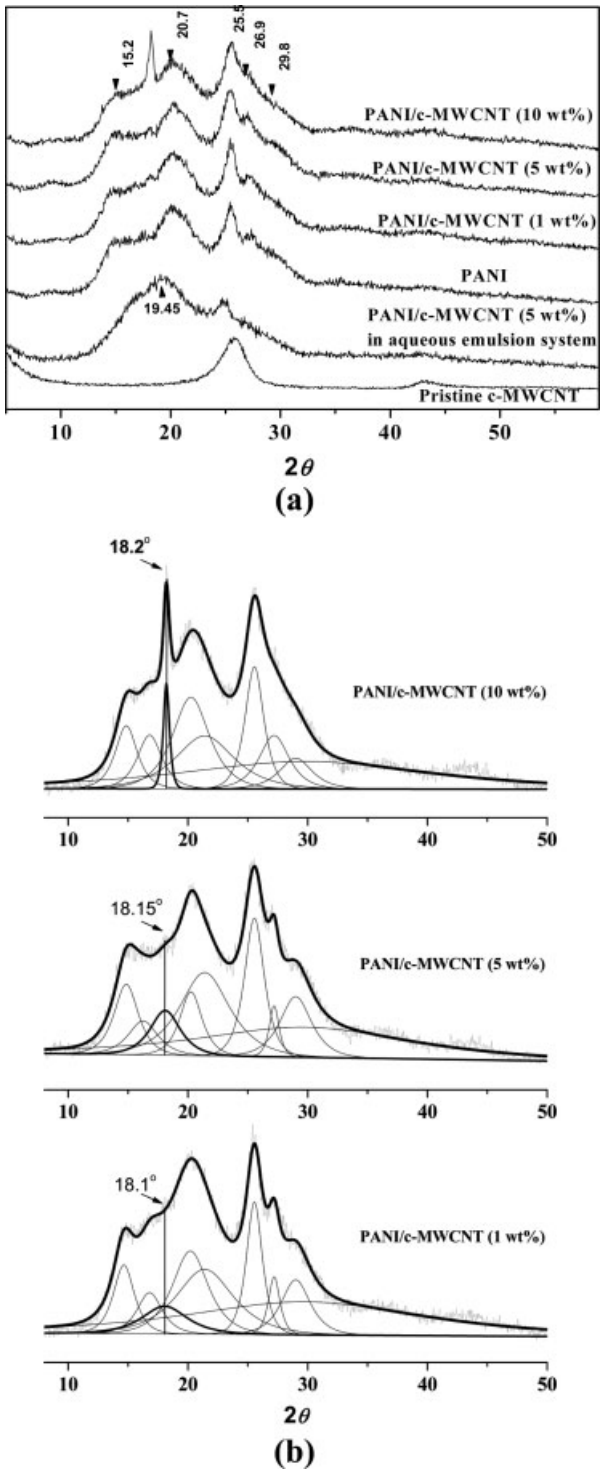

Figure 7. WAXD patterns of PANI/c-MWCNT composites with different amounts of c-MWCNT synthesized by inverse emulsion polymerization and aqueous emulsion polymerization (a); Resolved WAXD patterns of composites with different content of MWCNT (b).

Table 1. Profiles of Peak Near $2\theta = 18^\circ$ from Resolved WAXD Pattern of PANI/c-MWCNT Composite from Inverse Emulsion Polymerization According to c-MWCNT Content

c-MWCNT Content	1 wt %	5 wt %	10 wt %
Center of peak position	18.1°	18.15°	18.2°
Full width at half maximum (FWHM)	4.409	2.940	0.601
Crystal size (nm)	1.8	2.7	13.2

18.2°. This additional ordering is caused by different ordering of PANI near the surface of c-MWCNT. The mechanism of adhesion of PANI on the c-MWCNT surface is considered to be strong π–π attraction between the hexagonal surface lattice of the c-MWCNT and planar structured molecules of PANI. Maser and coworkers[41] supported the assumption for attraction force between PANI and MWCNT and shape of adhesion at interface by atomic force microscopy. The additional structural order could also be observed in the synthesis of poly(diphenylamine) (PDPA)/MWCNT composite by Lee and coworkers.[22] Neutral PDPA with aromatic amine exhibited no sharp peaks. However, there appeared two sharp peaks at 18.5° and 20.9° due to application of MWCNT. In our research, increase of the peak intensity near 18.2° was observed, as the c-MWCNT content was increased. More detailed characterization WAXD patterns were resolved as shown in Figure 7(b). The sharp shape of peak indicates that the periodicity became regular with increase of c-MWCNT. From the peak position and full width at half maximum (FWHM), the lattice size could be calculated (Table 1). Although each resolved peak near 18.2° centered almost same position, the FWHM became narrower with increase of c-MWCNT content. As a result, lattice size of the composite with 10 wt % MWCNT was observed to be grown. From this result, it could be concluded that the c-MWCNT act as template providing Van der Waals bonding site on which PANI molecules adhere regularly and the formation of composite was due to π–π attraction between the hexagonal surface lattice of the c-MWCNT and planar structured molecules of PANI not by simple aggregation between PANI molecules and c-MWCNTs.

Thermal Properties

As shown in Figure 8, the thermal stability of the composites was observed with different contents of c-MWCNT and DBSA using TGA. In thermograms of each sample, the first weight loss was observed between 250 and 350 °C, which is attributed to the loss of dopants from PANI/c-MWCNT composites (Region I). Another considerable weight loss was observed between 350 and 580 °C (Region II). This region of decomposition is assumed to be the degradation of the main chain of PANI. Finally, at temperatures above 580 °C, the steep slope decomposition curves indicate the decomposition of the backbone and ring opening of benzene (Region III).[35,42] The difference observed in Region I can be affected by dopant content. However, there was a significant difference between PANI/c-MWCNT and PANI with the same amount of DBSA. This result supports the effect of c-MWCNT on the formation of the highly ordered structure and the assumption of the existence of physical bonding between PANI and c-MWCNT. In Region II, the parallel slopes of the curves indicate that addition of c-MWCNT has no effect on the decomposition of the PANI main chains.

Compared with the composites from inverse emulsion polymerization, the product from aqueous emulsion polymerization exhibited a very high loss of weight in Region I. This high thermal weight loss indicates that the decomposed components included both dopant molecules and PANI matrix. This poor thermal stability was caused by the loose structure compared with the composite from inverse emulsion polymerization. These results agree with the analysis of WAXD patterns and support the highly ordered dense structure of PANI/c-MWCNT composite from inverse emulsion polymerization.

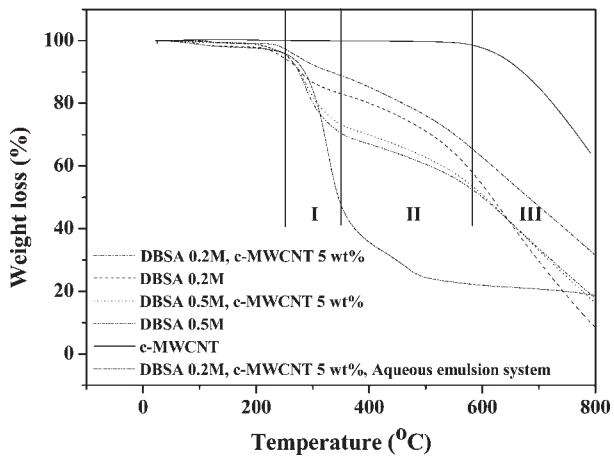

Figure 8. TGA diagrams of PANI/c-MWCNT composites with different contents of DBSA and c-MWCNT from inverse emulsion polymerization.

CONCLUSIONS

PANI/c-MWCNT composite doped with DBSA was synthesized successfully using inverse emulsion polymerization. As the content of c-MWCNT increased, the electrical conductivity of the composites increased and was higher than that from aqueous emulsion system. The increase of electrical conductivity results from the intrinsic electron transport capability of c-MCNT at the core of particles and the formation of a highly ordered structure of PANI molecules on the surface of c-MWCNT. This highly ordered structure has an advantage for intermolecular charge transport through overlap of π-orbitals between PANI molecules. The highly ordered structure was confirmed by characterization using WAXD patterns and TEM images. In the WAXD patterns, the crystalline peak of the composites from inverse emulsion polymerization appeared at higher angles than in the products from aqueous emulsion polymerization. As the content of c-MWCNT increased, the WAXD patterns of composites showed additional order of structures. TGA data showed better thermal stability of composites from inverse emulsion polymerization than those from conventional aqueous emulsion polymerization. The improvement in thermal stability results from the denser structure inhibiting evaporation of dopant molecules and the thermal decomposition of PANI.

Consequently, PANI/c-MWCNT composites prepared using inverse emulsion polymerization demonstrated better electrical and thermal properties than the composites from aqueous emulsion polymerization. This improvement is caused by the formation of a denser structure of highly ordered PANI molecules via inverse emulsion polymerization.

This research was supported by the research fund of Hanyang University (Grant No. HY-2007-I).

REFERENCES AND NOTES

1. Lee, K. H.; Cho, S. U.; Park, S. H.; Heeger, A. J.; Lee, C. W.; Lee, S. H. Nature 2006, 441, 65–68.
2. Kim, J. Y.; Kwon, S. C.; Han, S. W. Polym (Korea) 2003, 27, 549–554.
3. Jang, J.; Ha, J.; Kim, S. Macromol Res 2007, 15, 154–159.
4. Kaynak, A.; Wang, L.; Hurren, C.; Wang, X. Fiber Polym 2002, 3, 24–30.
5. Rhee, S. B.; Kim, H. K. J Kor Fib Soc 1984, 21, 115–125.
6. Kim, S. H.; Jang, S. H.; Byun, S. W.; Lee, J. Y.; Joo, J. S.; Jeong, S. H.; Park, M. J. J Appl Polym Sci 2003 87, 1969–1974.
7. Make, T.; Pienimaa, S.; Jussila, S.; Isotalo, H. Synth Met 1999, 101, 705–706.
8. Yussuf, A. A.; Sbarski, I.; Solomon, M.; Tran, N.; Hayes, J. P. J Mater Process Technol 2007, 189, 401–408.
9. Luzny, W.; Banka, E. Macromolecules 2000, 33, 425–432.
10. Chaudhari, H. K.; Kelkar D. S. Polym Int 1997, 42, 380–384.
11. Iijima, S. Nature 1991, 354, 56–58.
12. Kim, J. Y.; Han, S. I.; Kim, S. H. Polym Eng Sci 2007, 47, 1715–1723.
13. Kim, J. Y.; Park, H. S.; Kim, S. H. Polymer 2006, 47, 1379–1389.
14. Kim, J. Y.; Kim, S. H. J Polym Sci Part B: Polym Phys 2006, 44, 1062–1071.
15. Shin, Y. H.; Song, J. W.; Lee, E. S.; Han, C. S. Appl Surf Sci 2007, 253, 6872–6877.
16. Wu, T. M.; Lin Y. W. Polymer 2006, 47, 3576–3582.
17. Wei, Z.; Wan, M.; Lin, T.; Dai L. Liming Adv Mater 2003, 15, 136–139.
18. Zhou, Y. K.; He, B. L.; Zhou, W. J.; Huang, J.; Li, X. H.; Wu, B.; Li, H. L. Electrochim Acta 2004, 49, 257–262.
19. Huang, J. E.; Li, X. H.; Xu, J. C.; Li, H. L. Carbon 2003, 41, 2731–2736.
20. Feng, W.; Bai, X. D.; Lian, Y. Q.; Liang, J.; Wang, X. G.; Yoshino, K. Carbon 2003, 41, 1551–1557.
21. Markovic, M. G.; Matisons, J. G.; Cervini, R.; Simon, G. P.; Fredericks, P. M. Chem Mater 2006, 18, 6258–6262.
22. Showkat, A. M.; Lee, K. P.; Gopalan, A. I.; Kim, S. H.; Choi, S. H.; Sohn, S. H. J Appl Polym Sci 2006, 101, 3721–3729.
23. Sui, X.; Chu, Y.; Xing, S.; Liu, C. Mater Lett 2004, 58, 1255–1259.
24. Ichinohe, D.; Arai, T.; Kise, H. Synth Met 1997, 84, 75–76.
25. Rao, P. S.; Sathyanarayana, D. N.; Palaniappan, S. Macromolecules 2002, 35, 4988–4996.
26. Marie, E.; Rothe, R.; Antonietti, M.; Landfester, K. Macromolecules 2003, 36, 3967–3973.
27. Shreepathi, S.; Holze, R. Chem Mater 2005, 17, 4078–4085.
28. Han, D.; Chu, Y.; Yang, L.; Lv, Z. Colloids Surf A 2005, 259, 179–187.
29. Liang, Q.; Gao, L. Z.; Li, Q.; Tang, S. H.; Liu, B. C.; Yu, Z. L. Carbon 2001, 39, 897–903.
30. Chen, Y.; Shaw, D. T.; Guo, L. Appl Phys Lett 2000, 76, 2469–2471.
31. Sen, R.; Govindaraj, A.; Rao, C. N. R. Chem Phys Lett 1997, 267, 276–280.
32. Myers, D. Surface, Interfaces, and Colloids: Principles and Applications, 2nd ed.; John Wiley & Sons, Inc.: New York, USA, 1999.

33. Liu, J.; Rinler, A. G.; Dai, H. J.; Hafner, J. H.; Bradley, R. K. Science 1998, 280, 1253–1256.
34. Sun, Y. P.; Huang, W. J.; Lin, Y.; Fu, K. F.; Kitaygorodskiy, A.; Riddle, L. A.; Yu, Y.; Carroll, D. L. Chem Mater 2001, 13, 2864–2870.
35. Choi, J. H.; Kim, S. H.; Oh, K. W. Mol Cryst Liq Cryst 2007, 464, 281–289.
36. Chandrasekhar P. Conducting Polymers, Fundamentals and Applications: A Practical Approach; Kluwer Academic Publishers: Norwell, Massachusetts, USA, 1999.
37. Skotheim T. A.; Reynolds, J. R.; Conjugated Polymers: Theory, Synthesis, Properties and Characterization: Handbook of Conducting Polymers, 3rd ed.; CRC Press: New York, USA, 2007.
38. Kim, J. Y.; Kwon, S. J.; Ihm, D. W. Curr Appl Phys 2007, 7, 205–210.
39. Wu, T. M.; Lin Y. W.; Liao, C. S. Carbon 2005, 43, 734–740.
40. Liu, S. L.; Yue, J.; Wehmschulte, R. J. Nano Lett 2002, 2, 1439–1441.
41. Sainz, R.; Benito, A. M.; Martínez, M. T.; Galindo, J. F.; Sotres, J.; Baró, A. M.; Corraze, B.; Chauvet, O.; Maser, W. K. Adv Mater 2005, 17, 278–281.
42. Kim, S. H.; Oh, K. W.; Kim, T. K. J Appl Polym Sci 2005, 96, 1035–1042.